TECHNISCHE MECHANIK, 32, 2-5, (2012), 333 – 341
submitted: October 13, 2011

Fracture Toughness of Fibrous Membranes

C. T. Koh, M. L. Oyen

Random fibrous networks exist in both natural biological and engineering materials. While the nonlinear deformation of fibrous networks has been extensively studied, the understanding of their fracture behaviour is still incomplete. To study the fracture toughness of fibrous materials, the near-tip region is crucial because failure mechanisms such as fibril rupture occur in this region. The consideration of this region in fracture studies is, however, a difficult task because it involves microscopic mechanical responses at a small length scale. This paper extends our previous finite element analysis by incorporating the microscopic responses into a macroscopic domain by using a submodeling technique. The detailed study of microstructures at crack tips show a stochastic toughness of membranes due to the random nature of fibrous networks. Further, the sizes of crack tip region, which are sufficient to provide a reasonable prediction of fracture behaviour in a specific type of fibrous network, were presented. Future work includes improving the current linear assumption in the macroscopic models to become nonlinear.

1 Introduction

Biological materials such as the actin cytoskeleton in a cell (Lieleg et al., 2010), collagen in tissues (Kendra et al., 2010) and fibrin in blood clot (Brown et al., 2009), and engineering materials such as electrospun scaffolds (Blond et al., 2008) and paper materials (Isaksson, 2010), have microstructures in the form of random fibrous networks. The understanding of the fracture of these materials can not only facilitate the production of new materials with improved toughness, but also provides insights for new treatment of diseases and conditions that involve network failure. Despite its importance, the understanding of the fracture of fibrous materials is still incomplete. One of the main challenges is that fracture study involves multiple length scales: overall material failure at millimeter scale, nonlinear responses of fibrous networks at micrometer scale, and fibril rupture at nanometer scale.

The fracture toughness of fibrous materials has been studied by using various experimental and modeling techniques based on their length scales. For instance, the damage mechanisms of non-woven felts, which have fiber diameters approximately 15 μm, were studied by considering fibrous networks up to 10 mm; such study can considering microstructure responses in a length scale, that is comparable with the macroscopic length scale (Ridruejo et al., 2010). On the other hand, for fibrous materials, that have a small fiber diameter (e.g. micro-scale fiber diameter in paper (Hagglund and Isaksson, 2008); nano-scale fiber diameter in polymer (Treloar, 2009) and electrospun scaffold (Sundarrajan and Ramakrishna, 2007)), the consideration of fibrous networks up to millimeter scales requires large computational resources. The damage mechanisms of such materials have been studied by either only considering detailed study of fibrous networks in the near-tip region (Isaksson and Hagglund, 2007) or localized strain mapping at macro-scale without detailed consideration of fibrous networks (Stachewicz et al., 2011). In addition to these one-length-scale studies, two-length-scale studies such as modeling of effective-medium approximation of fibrous networks in a macroscopic domain have also been studied (Astrom and Niskanen, 1993).

The objective of the work presented here is to examine fracture behaviour of fibrous materials at two length scales. Finite element analysis was used to incoorperate microscopic responses in the crack-tip region into a macroscopic domain by using a submodeling technique. This modeling technique was compared to the technique, which applied K-dominant displacement fields at the outer mesh of microstructures, i.e. cross-linked fibrous networks. Detailed modeling of fibrous networks captures fiber ruptures, which cause cracks to start propagating. Further, the stochastic nature and size effect of fibrous networks were examined.

2 Finite Element Modeling at Two Length Scales

Mechanical responses of fibrous materials were studied at two length scales: the macroscopic model at millimeter scale and the microscopic model at micrometer scale (Figure 1). The macroscopic model consists of a strip with 25 mm width and 3 mm height, modeled by two-dimensional plane stress elements in finite element software ABAQUS (Version 6.11, SIMULIA, Providence, RI). It was pulled uniformly in vertical direction along the upper edge and constrained vertically at the bottom edge. Note that the width of the strip is approximately eight times greater than the height of the strip, and the length of the crack is approximately one third of the width of the strip. Such specimens exhibit fracture in shear-dominant responses (Genesky and Cohen, 2010). All simulations were performed using nonlinear finite element analysis, which considers large strains and rotations.

The microscopic models consist of two dimensional fibrous networks, constructed in circular unit cells. These fibrous networks were generated in MATLAB (The MatWorks, Natick, MA) by constructing lines from random points with random angles. The cross-linked fibrous networks were modeled by rigid bonding at all intersection points among fibrils. The fibrils were modeled with a length of 10 μm. However, these fibrils were cut whenever they exceeded the model cell edges. Further, a radius-length notch was assigned in the circular fibrous networks by cutting the fibrils that cross the notch path.

The network properties including fibril modulus $E_f = 100\,\mathrm{MPa}$, cross-link density $\rho_{density} = 2.35 \pm 0.15\,\mu m^{-2}$ and fibril diameter $d_f = 50\,\mathrm{nm}$ (Oyen et al., 2005) are representative of collagenous networks in amnion (i.e. a thin collagenous membrane continuous with the placenta (Oyen et al., 2004)). However, the networks presented here have two features (i.e. fiber length and bonding condition) slightly different than in amnion (Koh and Oyen, 2011). The fibrils were modeled by less than 1 μm length beam elements in ABAQUS. The beams were defined by stretching stiffness μ (i.e. axial force needed to stretch a unit axial strain) and bending stiffness κ (i.e. bending moment needed to bend a unit radius of curvature). A noodle-like behavior resembling collagen fibrils was defined: the fibrils were very easy to bend (μ = 1x10^{-15} Nm^2) but difficult to stretch (κ = 5 N). Both the stretching and bending stiffness depend not only on the Young's modulus but also the cross-sectional area of fibrils (Onck et al., 2005).

The macroscopic model was linked with microscopic models by a submodeling technique. First, the macroscopic model was simulated to obtain the macroscopic responses at the crack tip field. Then, the displacement field obtained from the macroscopic model was further assigned as the applied displacement of the microscopic models. Note that the macroscopic model was modeled in the mesh, which the nodes were matched with the microscopic models at the boundaries. Furthermore, nonlinear fracture responses of fibrous networks was studied by applying a displacement at the outer boundary of the circular fibrous meshes (Koh and Oyen, 2011). The imposed displacement components $(u_1,\, u_2)$ were based on linear elastic fracture mechanics (LEFM) and were expressed in terms of the polar co-ordinates $(r,\, \theta)$ as (Kanninen and Popelar, 1985):

$$u_1 = \frac{1}{2}\sqrt{\frac{r}{2\pi}}\frac{K_I}{G}(\kappa + 1 + 2cos^2\frac{\theta}{2})sin\frac{\theta}{2} \tag{1}$$

$$u_2 = \frac{1}{2}\sqrt{\frac{r}{2\pi}}\frac{K_I}{G}(-\kappa + 1 + 2sin^2\frac{\theta}{2})cos\frac{\theta}{2} \tag{2}$$

where K_I is the mode I stress intensity factor and *G* is shear modulus. The fibrous networks are assumed to be in plane stress by having $\kappa = (3-\nu)/(1+\nu)$ with Poisson's ratio $\nu = 0.3$. The shear modulus *G* was defined as 4 MPa. As the displacement fields obtained from the macroscopic model shall be in a good agreement with Eq. (1) and Eq. (2), the nonlinear responses of fibrous networks are expected to be similar for our previous and current modelling approaches, but this was tested explicitly here.

The failure criterion was defined as following: a fiber ruptures whenever local stress exceeds the tensile fracture strength of fibrils, defined as $\sigma_f = 30\ MPa$. The experimental measurements of the fracture strength of collagen fibrils vary from 20 MPa to 600 MPa (Grant et al., 2008). In ABAQUS, failure (e.g. critical crack opening) was determined whenever the local maximum stress of fibrils reached the strength of fiber. These local maximum stresses were, however, not a fixed value; they have an overshoot (30 – 32 MPa as shown in table 1) due to discrete time steps in ABAQUS. The critical crack opening was obtained when the first fibril ruptures and allows crack propagation.

The size of the crack-tip region in a network was studied by simulating microscopic models with four radii: 3 μm, 6.25 μm, 12.5 μm and 25 μm. These different sizes of circular networks were obtained from the same master network and thus had the same network configuration at the crack tip (figure 2). The nodes at the periphery of the circle were used as the boundary nodes to connect to the macroscopic model. Furthermore, four additional networks which followed the same randomization procedure were generated with 25 μm in radius, to study the stochastic nature of different random fibrous networks. The stochastic properties among these networks as shown in Table 1 include (1) stochastic fiber density, i.e. sum of fiber length per unit area, and (2) cross-link density, i.e. sum of cross-links per unit area.

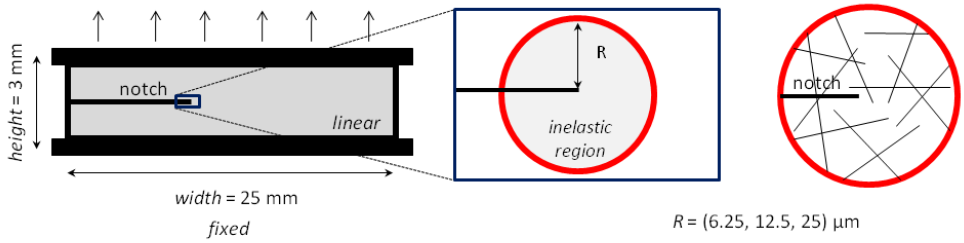

Figure 1: Schematic illustraion of the inelastic region (middle) in the macroscopic models (left) and the fibrous networks in the microscopic models (right).

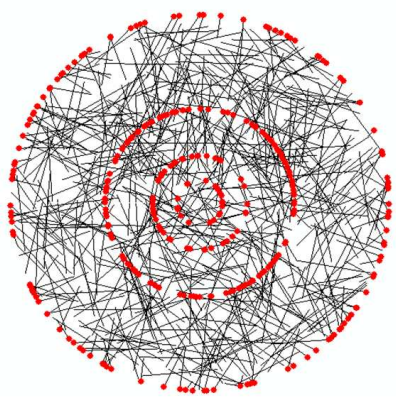

Figure 2: Mesh and boundary nodes (highlighted in red (dots)) in the microscopic models of radii $R = (3,\ 6.25,\ 12.5,\ 25)\ \mu m$.

Networks	Fiber density (mm^{-1})	Cross-link density (μm^{-1})	Maximum stress (MPa)
1	2746.2	2.4665	29.96
2	2773.9	2.4421	31.05
3	2783.6	2.4619	30.01
4	2703.3	2.3922	32.17

Table 1: Fiber density, cross-link density and actual maximum stress at critical crack opening of four random fibrous networks.

3 Results

3.1 Failure at Crack Tip

Figure 3 shows the initial mesh and the stress distribution of the crack-tip region in macroscopic model at macroscopic crack opening $\delta_\infty/h = 0.024$. Different crack-tip region sizes, i.e. radius $R = (3,\, 6.25,\, 12.5,\, 25)\,\mu m$, studied in this paper are highlighted with red lines. Note that the displacement of nodes which were located at these lines was used as the applied displacement of the microscopic models.

Figure 4 shows the undeformed and deformed fibrous networks with four different model sizes when the crack starts propagating. Note that these networks have approximately the same cross-link density. Each of them has size twice larger than the network on the left. The stress at the crack tip predicted by the macroscopic model (both S_{xx} and S_{yy}) is smaller than the prediction of microscopic models. The stress distribution indicated in fibrous networks is the stress of individual fibril. The maximum stress occurred at the crack tips and this stress would have caused the fibril to rupture. The maximum stress always occur in tension rather compression. Fibrils, which have very small bending stiffness, bent rather than compressed.

Figure 5 shows that the maximum stress of fibers in fibrous networks was increased when the crack opening increased. The fiber strength $\sigma_f = 30\,\mathrm{MPa}$ indicates the initiation of crack propagation. The crack starts propagating at the corresponding macroscopic crack opening (δ_∞/h) of approximate 0.02125. By comparing the network with different sizes, the fibrous network with radius $R = 3\,\mu m$ exhibits significantly larger maximum stress than the fibrous networks with radius $R = (6.25,\, 12.5,\, 25)\,\mu m$. Note that the large radius fibrous networks i.e. $R = (6.25,\, 12.5,\, 25)\,\mu m$ exhibit a consistent prediction of maximum stress. On the other hand, there is a variation in maximum stress among four random fibrous networks of size $R = 25\,\mu m$ due to the stochastic nature of the networks.

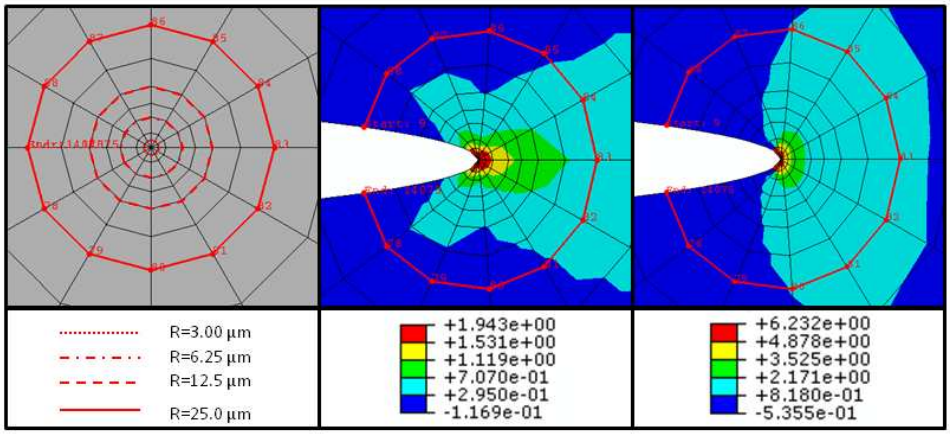

Figure 3: The initial configuration (left), stress distribution S_{xx} (middle), and stress distribution S_{yy} (right) of the crack-tip region in the macroscopic model. The red lines indicate four sizes of crack-tip regions studied in this paper.

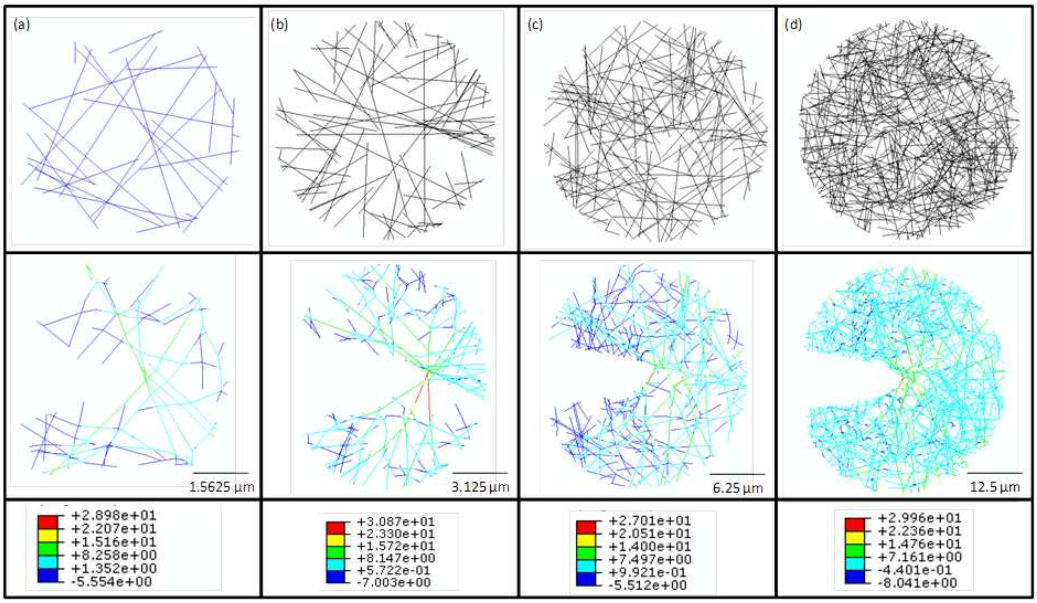

Figure 4: The undeformed (upper) and deformed (lower) fibrous networks at critical crack openings, with model radii: (a) $R = 3.0\,\mu m$, (b) $R = 6.25\,\mu m$, (c) $R = 12.5\,\mu m$ and (d) $R = 25.0\,\mu m$.

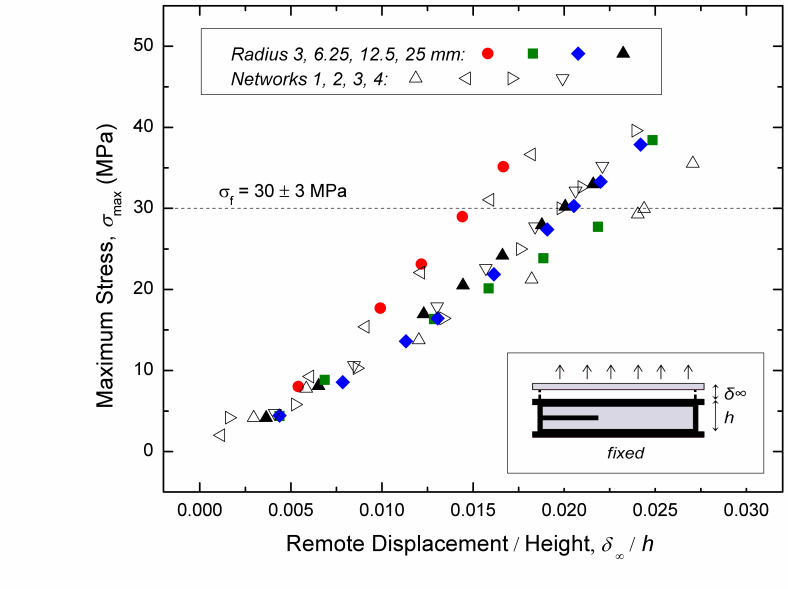

Figure 5: Maximum stress of fibrils in the fibrous networks predicted by the microscopic models with different radius and different random networks.

3.2 Critical Crack Openings

Figure 6 shows the critical crack openings, i.e. the notch opening profile when crack starts propagating. These crack openings were obtained whenever a fiber in the microscopic models reached the assigned fiber strength. The corresponding macroscopic responses when a crack starts propagating were also shown. The comparisons shown in figure 6 include (1) the prediction of the two-length-scale models using a submodeling technique versus the prediction of our previous models (Koh and Oyen, 2011) by applying the K-displacement fields at the outer mesh, which was based on LEFM, (2) the prediction of the macroscopic model versus of the microscopic models, and (3) the variation among responses of fibrous networks generated by the same randomization procedure. First, the submodeling technique provide similar predictions as the LEFM equation technique. Second, the critical crack opening predicted by the macroscopic model and the microscopic model are similar. However, note that the critical crack opening profiles of the macroscopic model were obtained based on the corresponding responses of the microscopic models. Third, there is a significant variation among different random networks; this difference is similar to the variation of the maximum stress of fibrous networks (figure 5), which determines the network failure.

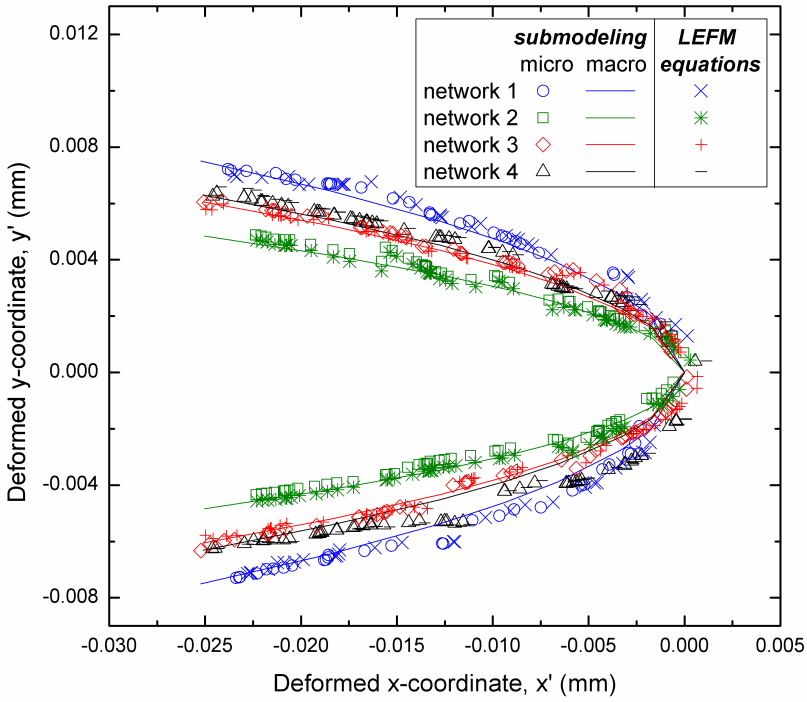

Figure 6: The comparison of critical crack opening profiles stochastic fibrous networks, predicted by the macroscopic model and microscopic models using a submodeling technique, and the LEFM-equation approach.

3.3 Energy Analysis

Figure 7 shows the strain energy of fibrous networks, which was calculated from microscopic models with different radius and different random networks. The strain energy was increased when the crack opening was increased. Microscopic models with radius $R = (3,\ 6.25,\ 12.5,\ 25)\,\mu m$ predicted similar strain energy per notch length (U/L_n). Most of the predictions have similar U/L_n curves, but there is a significant variation among the predictions. Networks 1, 2 and 3, which have approximately values identical of fiber density (table 1), have similar energy curves while network 4, which has a smaller fiber density, has a substantially different strain energy curve. This variation becomes more apparent when the crack opening increases.

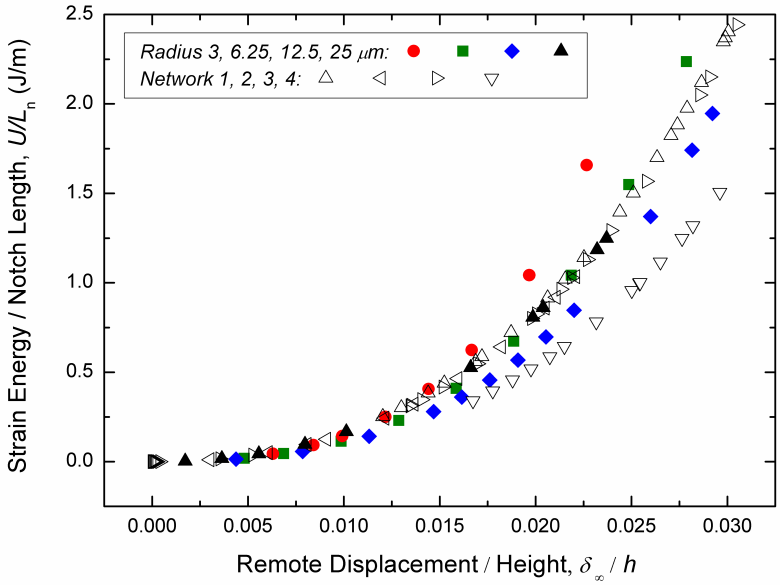

Figure 7: Strain energy of fibrous networks predicted in microscopic models with different radius and different networks.

4 Discussion

4.1 Stochastic Toughness

Due to the singular nature of the elastic stress field, the crack-tip region responds mechanically in an inelastic manner, where the processes of fiber rupture and bond breakage occurs (figure 1 (middle)). Within this region, the linear elastic solution is invalid (Livne et al., 2010). The fracture criterion defined in continuum mechanics considers particular components of the stress or strain tensor at the crack tips. The definition of such a fracture criterion hardly captures the physical failure of the material, mainly because failure happens at a smaller scale than the continuum elements. This study therefore considers the detailed study of microstructures at crack-tips and defines failure based on a physical basis, i.e. fiber rupture.

A region surrounding this nonlinear crack-tip region is known as the K-dominant region, which exhibits linear responses and can be described by the stress intensity factor $K = K(\sigma, a)$ (Kanninen and Popelar, 1985). Based on LEFM, by describing the mechanical responses with stress intensity factors, the K-dominant region is directly connected to the far-field displacement in the macroscopic domain. The prediction of a submodeling technique is in good agreement with the prediction of LEFM-equation approach. However, both the submodeling technique and the LEFM-equation approach assume the materials respond linearly elastic in macroscopic scale, but many fibrous materials including biological polymers and rubber-like materials exhibit nonlinear strain stiffening behaviours (Kendra et al., 2010). The invalidity of linear assumption in fibrous materials motivates further work to consider nonlinear behaviour in the macroscopic domain.

The stochastic nature of fracture toughness of the fibrous materials were observed in (1) maximum stress at critical crack opening (figure 5), (2) critical crack opening profiles (figure 6), and (3) strain energy (figure 7). These variations result from four main factors. First, the variation of network topology (e.g. fiber orientation and fiber length between two cross-links) at the crack tips results in different maximum stress across networks. Second, the variation of fiber density (table 1) resulted from the variation of the total fiber length in the microscopic models, and further influenced the variation of strain energy. Third, the cross-link density can affect the deformation of fibrous networks and thus its variation (table 1) contributed to the stochastic nature of fracture toughness. Fourth, the maximum local stress which determines the critical crack opening has an overshoot due to discrete time steps in ABAQUS.

4.2 The Size of Microscopic Models

In order to eliminate any variation caused by different stochastic random networks, the fibrous networks with four different radii presented here were obtained from the same network and have the same fibril configuration at the crack tip. The size of microscopic models were studied by comparing their maximum stress (figure 5) and strain energy. Fibrous networks with radius R = 6.25 μm, R = 12.5 μm and R = 25 μm exhibit similar quantitative values in both maximum stress and strain energy while fibrous network with radius R = 3 μm exhibited different values from the rest of the networks. This suggests that the continuum assumption at crack tip region smaller than 3 μm is physically unrealistic. A crack tip region with a radius larger than 6.25 μm is sufficient to provide a reasonable prediction of fracture behavior.

The material toughness can be quantified by the energy needed to initiate crack propagation. The total energy *U* of the fibrous networks can be described as $U = U_{\mathrm{A}} + U_{\mathrm{E}} + U_{\mathrm{S}}$ where U_{A} is the potential energy of the applied boundary conditions at the periphery, U_{E} is the strain potential energy stored in deformed fibrous networks and U_{S} is the free energy expended in creating the new crack surfaces. Based on the Griffith energy balance concept, fibrous networks with crack length c are in equilibrium by the means of $dU/dc = 0$. During crack propagation with creation of new fracture surfaces, the mechanical energy decreases ($d(U_{\mathrm{A}} + U_{\mathrm{E}})/dc < 0$) while the surface energy increases ($dU_{\mathrm{S}}/dc > 0$). A crack would extend when dU/dc was negative (Lawn, 1998). Similar strain energy per notch length (U/L_n) for microscopic models with radius *R* = 6.25 μm, *R* = 12.5 μm and *R* = 25 μm suggest similar predictions for toughness.

5 Conclusions

The submodeling technique used in the finite element analysis is able to capture the stochastic nature of failure mechanisms, i.e. fiber ruptures at the crack tips. The modeling represented in this paper was compared with our previous study, which investigated nonlinear responses of fibrous networks by applying K-dominant displacement fields. Both the current and previous studies are suitable for materials which exhibit linear behavior at macroscopic scale. Future work will involve relaxing the linear assumption to utilize a nonlinear response in the macroscopic domain. Further, the microscopic model with a small radius (*R* = 6.25 μm) can capture similar failure behavior as the microscopic model with a large radius (*R* = 25 μm); such understanding provides a guideline to help reduce computational usage in future studies of microstructurally controlled fracture.

References

Astrom, J. A.; Niskanen, K. J.: Symmetry-Breaking Fracture in Random Fibre Networks . *Europhysics Letters*, 557.

Blond, B. D.; Walshe, W.; Young, K.; Blighe, F. M.; Khan, U.; Carpenter, L.; Mccauley, J.; Blau, W. J.; Coleman, J. N.: Strong , Tough , Electrospun Polymer - Nanotube Composite Membranes with Extremely Low Density. *Advanced Functional Materials*, 18, (2008), 2618–2624.

Brown, A. E. X.; Litvinov, R. I.; Discher, D. E.; Purohit, P. K.; Weisel, J. W.: Multiscale mechanics of fibrin polymer: gel stretching with protein unfolding and loss of water. *Science*, 325, 5941, (2009), 741–4.

Genesky, G. D.; Cohen, C.: Toughness and fracture energy of PDMS bimodal and trimodal networks with widely separated precursor molar masses. *Polymer*, 51, 18, (2010), 4152–4159.

Grant, C. A.; Brockwell, D. J.; Radford, S. E.; Thomson, N. H.: Effects of hydration on the mechanical response of individual collagen fibrils. *Applied Physics Letters*, 92, 233902.

Hagglund, R.; Isaksson, P.: On the coupling between macroscopic material degradation and interfiber bond fracture in an idealized fiber network. *International Journal of Solids and Structures*, 45, (2008), 868–878.

Isaksson, P.: An implicit stress gradient plasticity model for describing mechanical behavior of planar fiber networks on a macroscopic scale. *Engineering Fracture Mechanics*, 77, 8, (2010), 1240–1252.

Isaksson, P.; Hagglund, R.: Evolution of bond fractures in a randomly distributed fiber network. *International Journal of Solids and Structures*, 44, (2007), 6135–6147.

Kanninen, M. F.; Popelar, C. H.: *Advanced Fracture Mechanics*. Oxford University Press (1985).

Kendra, A. E.; Henderson, K. J.; Shull, K. R.: Strain Stiffening in Synthetic and Biopolymer Networks. *Biomacromolecules*, 11, 5, (2010), 1358–1363.

Koh, C.; Oyen, M. L.: Branching Toughens Fibrous Networks. *Journal of the Mechanical Behavior of Biomedical Materials. Submitted (2011)*.

Lawn, B.: *Fracture of Birttle Solids*. Cambridge University Press, second edi edn. (1998).

Lieleg, O.; Claessens, M. M. a. E.; Bausch, A. R.: Structure and dynamics of cross-linked actin networks. *Soft Matter*, 6, 2, (2010), 218.

Livne, A.; Bouchbinder, E.; Svetlizky, I.; Fineberg, J.: The near-tip fields of fast cracks. *Science*, 327, 5971, (2010), 1359–63.

Onck, P. R.; Koeman, T.; Dillen, T.; Giessen, E.: Alternative explanation of stiffening in cross-linked semiflexible networks. *Phys. Rev. Lett.*, 95, 17, (2005), 178102.

Oyen, M. L.; Calvin, S. E.; Cook, R. F.: Uniaxial stress-relaxation and stress-strain responses of human amnion. *Journal of materials science. Materials in medicine*, 15, 5, (2004), 619–24.

Oyen, M. L.; Cook, R. F.; Stylianopoulos, T.; Barocas, V. H.; Calvin, S. E.; Landers, D. V.: Uniaxial and biaxial mechanical behavior of human amnion. *Journal of Materials Research*, 20, 11, (2005), 2902–2909.

Ridruejo, A.; González, C.; LLorca, J.: Damage micromechanisms and notch sensitivity of glass-fiber non-woven felts: An experimental and numerical study. *Journal of the Mechanics and Physics of Solids*, 58, 10, (2010), 1628–1645.

Stachewicz, U.; Peker, I.; Tu, W.; Barber, A. H.: Stress delocalization in crack tolerant electrospun nanofiber networks. *ACS applied materials & interfaces*, 3, 6, (2011), 1991–6.

Sundarrajan, S.; Ramakrishna, S.: Fabrication of nanocomposite membranes from nanofibers and nanoparticles for protection against chemical warfare stimulants. *Journal of Materials Science*, 42, 20, (2007), 8400–8407.

Treloar, L. R. G.: *The Physics of Rubber Elasticity*. Oxford University Press, third edit edn. (2009).

Address: Ching Theng Koh, Engineering Department Cambridge University, Trumpington Street, Cambridge CB2 1PZ, U.K.; University of Tun Hussein Onn Malaysia, 81310 Parit Raja, Johor, Malaysia
Dr. Michelle L. Oyen, Engineering Department Cambridge University, Trumpington Street, Cambridge CB2 1PZ, U.K.
email: ctk24@cam.ac.uk;mlo24@cam.ac.uk